Dynamic weather effects induced from the 2017 total solar eclipse

Bianca Pina* and Paul Ronquillo†
Arizona State University, Tempe, Arizona, 85287

Thomas G. Sharp‡
Arizona State University - School of Earth and Space Exploration, Tempe, Arizona, 85287

This research project was part of a nationwide effort organized by Montana Space Grant Consortium to study and image the 2017 total solar eclipse with high altitude balloons. Our mission was to measure the changes in light from the total solar eclipse and its effects on the local weather conditions in the air and on the ground. Our results showed that the effects of totality on the ambient light levels were gradual until 90 seconds before totality when light levels decreased sharply. Air temperature and pressure decreased throughout the eclipse as a result of the loss of sunlight. A short-term pressure increase, associated with totality, was measured at our ground station. We propose that this localized high-pressure event is the result of a column of sinking cold air around the umbra.

I. Introduction

This research project was part of a nationwide effort organized by Montana Space Grant consortium to study and the 2017 total solar eclipse with high altitude balloons. Each participating Space Grant consortium deployed a primary payload for collecting and transmitting live video and a secondary scientific payload with the science objectives defined by the student payload team. Embry Riddle Aeronautical University provided the primary payload and communication ground station and we (Arizona State University) provided the science payload. It has been observed that a solar eclipse will induce noticeable weather changes including sharp drops in temperature, pressure fluctuations and changes in wind direction[1,3,4.] Our mission was to measure the changes in light through the total solar eclipse and its effects on the local weather conditions in the atmosphere and on the ground. Specifically, we set out to measure changes in temperature, pressure and humidity associated with the eclipse, including the sudden transition to totality. In addition, we deployed a thermal imaging camera on our payload to capture infra-red images of the ground during the eclipse to provide a real view of the temperature changes on the ground. We also established a ground weather station to collect complementary light, temperature, pressure and humidity data during the eclipse that could be compared to the flight data.

II. Methods

A. Science Methods

To better understand how the solar eclipse affects the atmosphere, we established a ground weather station to provide context to our payload data during the flight.

1. Determining Mission Design

To measure the temperature, we flew a resistance-based RTD Sensor. This sensor is accurate and provides temperature data in sub-zero temperature conditions. The RTD operates over a range of -200 to 550 degrees Celsius. We also incorporated a DHT22 Temperature/Humidity sensor to provide humidity data and compliment the RTD. The DHT22 is a capacitance based humidity sensor which can be unreliable at freezing temperatures because of a reliance on the liquid phase of water. To measure absolute pressure, we used an Adafruit MPL3115A2 Pressure/Altitude Sensor. This sensor records the absolute pressure and calculates altitude with temperature compensation. A Venus GPS receiver was used

*Science Research Lead, Arizona State University - School of Earth and Space Exploration, 781 S Terrace Rd, Tempe, Arizona, 85287
†Engineering Lead, Arizona State University - Ira A. Fulton Schools of Engineering, 699 S Mill Ave, Tempe, Arizona, 85281
‡Mentor, Arizona State University - School of Earth and Space Exploration, 781 S Terrace Rd, Tempe, Arizona, 85287

for accurate 3D location. To measure light level changes throughout the eclipse, we incorporated a Lux Sensor and a UV Sensor which contained photodiodes sensitive to visible, infrared, and ultra-violet wavelengths, separately. To measure payload orientations and accelerations during the flight, we incorporated an Adafruit Precision NXP 9 Degrees of Freedom accelerometer/gyroscope/magnetometer sensor. This sensor was used to calculate AHRS orientation and provide context for the physical flight conditions and the direction the payload sensors are facing.

2. Determining Ground Station Requirements

For ground-level weather data and context to the balloon data, we built a weather station with a similar sensor array to that of the balloon payload. For the ground weather station, we used a Sparkfun weather shield that attached to a resistor ladder wind vane and cup anemometer. The weather shield contained a GPS, temperature, humidity, light, and pressure sensors. The Si7021 temperature/humidity sensor uses a silicon band-gap for temperature and a capacitance based humidity sensor. The light sensor aboard the shield used an ALS-PT19 ambient light sensor mainly sensitive to the visible spectrum. The wind vane, attached to the weather shield, used a resistive wind vane and cup anemometer to measure wind speed and direction.

B. Engineering Methods

The engineering requirements to complete this payload were split off into two sections: The Computer Electronics and the Structure.

1. Computer Engineering with Arduino

The eclipse totality was expected to be about two minutes long, which suggests that the weather changes would be short lived and small in magnitude compared to the full weather balloon flight. To maximize our data collection during totality and increase the chances of measuring small weather fluctuations, we chose an Arduino Due for the system master controller for its high memory clock speed. The Arduino Due has a large memory at 512 kb and fast CPU speed at 84MHz to provide high temporal data resolution through the flight. This helped increase the data logging frequency up to 1 data point every 2 seconds rather than every 9 seconds or more if we had used an Arduino UNO. The majority of the payload sensors array is fed into the central controller through SPI, I2C, UART, and Dallas Semiconductor 1-Wire serial protocols in addition to two analog temperature sensors for measuring payload internal temperature. The pressure and two light sensors were separated from the main controller and its sensor array because of interference with other sensors and the Arduino Due's implementation of the I2C repeated-start condition. Those sensors were controlled by two slave Arduino UNOs that fed the sensor data back to the central controller for logging to a CSV file. The main electronics system was fabricated by separating the payload sensors into devices that require access to outside the payload walls and those that do not. An Arduino Mega protoshield, a premade Arduino Mega shaped perforated PCB, was then used to mount sensor boards and locking cables for sensors measuring the outside of the payload housing. Sensors that require access to the environment outside the payload are fastened to the outside payload walls using adhesive and screws or mounted over port holes drilled into the wall material. This system utilizes two separated electrical systems with separate power supplies, a controller system running the sensors, and a dedicated power supply for the thermal camera. The three processors and sensor array are powered by a 2AH 3.7V lithium battery regulated by a boost-buck power regulator raising the regulated power to 5V and providing an approximated eight hours of battery life. The thermal camera is powered by four AA lithium batteries with power systems wired to unique key-switches as single points of startup for the systems.

2. Mechanical Engineering

The payload housing consists of a hardened resin impregnated carbon fiber cylinder wall with two Lexan poly-carbonate plates sealing the top and bottom of the cylindrical body. The carbon fiber walls have threaded rod struts for fastening the poly carbonate lids to the cylinder. Going through the center of the payload is a threaded brass rod which is attached to the balloon tether with hitch pins. Inside of the payload is a third Lexan plate used for mounting the main controller system and physically separating the camera and its power from the main system. The center plate is held in place by nuts and washers with thread-lock adhesive on the central threaded rod, and silicone caulk around the edge to create a seal between the plate and the payload wall. To avoid over heating of the payload from the heat generated from the IR camera, ventilation holes were added to the camera chamber. Sensors that needed external access, including the humidity, temperature and pressure sensors, were mounted externally with bolts and adhesive or mounted

internally over holes for exposing the active portion of the sensor. Since the other internal temperature sensor was for the controller, it is left with short leads soldered directly to the shield. The camera is mounted in a downward facing direction using a GoPro camera mount bolted to the carbon fiber wall with holes drilled into the Lexan for the visible and IR camera lenses.

C. Challenges

The major challenge for this design was a faulty implementation of the I2C protocol repeat-start condition in the Arduino Due controller itself. This signal, made between the master and slave device, is used for sending configuration data to sensors prior to reading. Any sensor using the repeat-start feature either can't be seen or configured by the master. Part of the solution was editing the I2C source files used by the Arduino Due and changing the affected sensor libraries to match this change. This worked for most of the sensors using this protocol except for the altimeter, utilizing a slightly different I2C control style. An additional problem with the altimeter is that it requires about two seconds to read data, which makes it a bottleneck for the system speed. To work around these problems with the Arduino Due, the pressure and light sensors were run on separate Arduino UNO controllers, which passed their data to the master controller when called on. This was done using a pull up resistor to connect a slave select signal from the master to the slave controllers, and then transmitting the actual sensor data using a UART serial transmission. The IR camera, which has a peak power of 3.3 Watts, had to be separated from the rest of system sensors into a different chamber. Without ventilation, the camera chamber quickly reaches temperatures up to 140F. The heat produced by the camera was also a problem for IR imaging. In the initial design, the camera was mounted inside the Lexan plate, which is transparent for most of the wavelengths we were measuring. However, the hot Lexan reflected so much heat back to the camera that no external heat signatures were visible. To solve this problem, port holes were added for both visible and IR lenses. To assist with cooling the camera chamber, two quarter inch diameter holes were drilled into the sides of the chamber for ventilation.

III. Results

A. Weather Station

The weather ground station was located at our base camp at the Reno Cove campsite in Glendo State Park, outside of Glendo, Wyoming. The ground station was in open sunlight to measure changes in light directly. However, this resulted in temperature readings that were significantly higher than ambient air temperatures. The data (Figure 1) shows the striking change in light levels during the solar eclipse. The measured voltage from our light sensor starts at 3.21 V, which was near the 3.3 V maximum before the eclipse, decreased by about 5% percent during the hour-long transition through the penumbra before plummeting and additional 95% to 0.0 V at the onset of totality. The sudden transition to darkness occurred in 90 seconds. The ground station temperature declined steadily from 40.5 °C through the eclipse and reached a minimum of 21.1 °C at the end of totality. When the light returned temperatures rose to 46.1 °C. The relative humidity, which is inversely related to temperature, increased through the eclipse totality before decreasing again after totality. The ambient air pressure decreases by 289 Pa before totality and then increases by 293 Pa after totality, but with a 120 Pa local pressure peak centered at totality. At 10:36:13 AM, 8 minutes and 51 seconds before totality, the pressure started to increase, reaching a maximum pressure of 85,554 Pa 10 seconds after totality. The pressure then dropped back down to 85434 Pa at 10:56:24, about 9 minutes after the end of totality. The total duration of this pressure pulse was 20 minutes and 11 seconds.

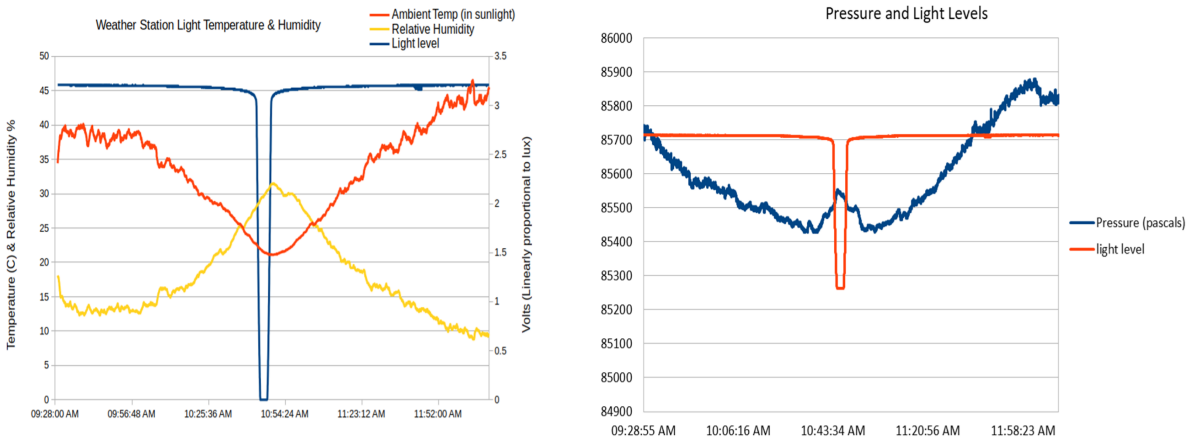

(a) **(b)**

Fig. 1 Plots of recorded weather station light, temperature, relative humidity and pressure during the solar eclipse event. The light curve illustrated the onset of totality as a rapid drop in light level, followed by symmetric increase at the end of totality.

B. Payload

The balloon was launched from Laramie Peak Scout Camp, approximately 25 miles southwest of our ground station at Glendo State Park. Our payload was launched at 10:20:09am on the second of two balloons. The easterly flight path took the balloon south of our ground station, landing approximately 25 miles east of Glendo (Figure 2). The payload passed through the eclipse totality during the assent, between 37,000 ft. and 40,000 ft. As a result of complications at the launch site, the launch was delayed by 32 minutes from the intended launch time and our payload passed through eclipse totality at about 30k ft. below the intended altitude for our measurements. The balloon had an average ascent rate of 10.8mph and reached its peak altitude of 100,000 ft. at 11:59:05 am, when it burst and the payload train started its of 37.5 minute descent. Altitude was measured by GPS and by barometric altimeter. An apparent malfunction in the altimeter resulted in peak altitude reading of only half of that measured by GPS. The entire flight lasted 2 hour and 16 minutes. The initial descent of the payloads involves a violent near free fall immediately after balloon burst. Three-axis accelerometer data (Figure 3a) shows a steady ascent, followed by a sudden increase in accelerations up to 40 m/s2. Payload accelerations decrease significantly at about halfway through the decent and then increase again near the end of the flight. Accelerations cease when the payload is stationary on the ground.

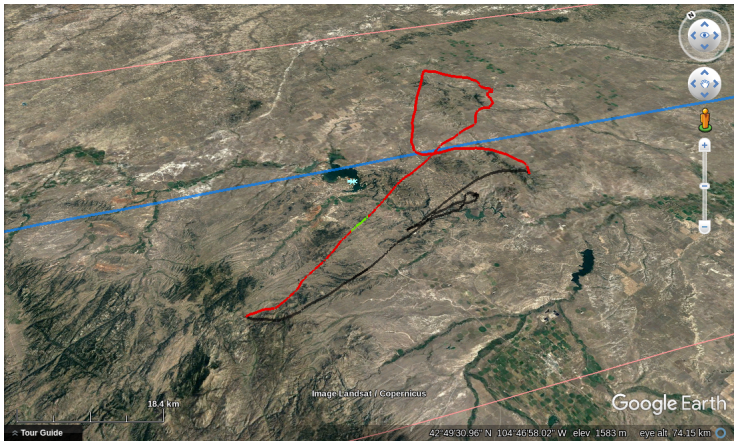

Fig. 2 3D model of the flight path taken by our payload with respect to the weather station (marked in light blue). The flight path through totality is marked in dark blue. The flight followed an ENE path until it reached about 80,000 feet where it reversed its trend until burst at 100,000 ft. A projection of the flight path on the ground is marked in black.

Changes in measured light levels provided a means of determining the exact time of totality experienced by our payload. Light levels measured in visible, infrared and lux was constantly changing during the flight because of the changing orientation of the payload relative to the sun. To pinpoint the time of totality, we examined the change in light levels (dLux/dt) versus time (figure 3b) to find time stamps that correspond to zero variation and low light levels. These measurements indicate that the payload passed through totality from 10:44:57 AM to 10:47:12 AM, a duration time of 2 min 15s, during the assent between 37,000 ft. and 40,000 ft.

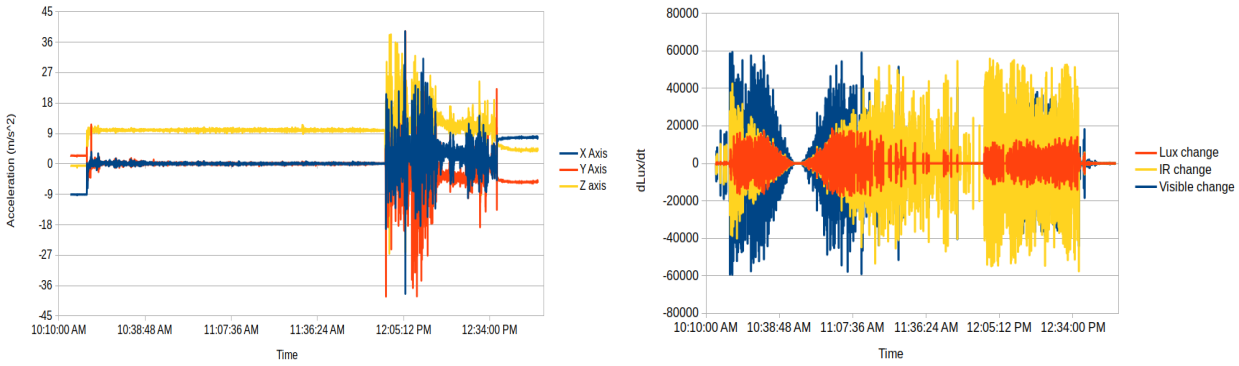

(a) **(b)**

Fig. 3 Payload acceleration (a) and light level data (b) plots. (Figure 3a) shows X (blue) Y (red) and Z (yellow) acceleration $\frac{m}{s^2}$ versus time, illustrating the motion of the payload during the flight. After constant low accelerations, the time of balloon burst is marked by a rapid increase in acceleration up to 40 $\frac{m}{s^2}$ until a 18 $\frac{m}{s^2}$ acceleration impact with the ground. (Figure 3b) plots the change in light levels for our Lux (red), IR (yellow) and visible (blue) light sensors. These changes in light decrease during the eclipse as totality is approached and they fall to zero variation during totality. This approach provides and exact time of totality from the payload.

Based off of a simple temperature model of the atmosphere[2.], the measured values and the expected values of the temperature profiles were plotted together (Figure 4a). The expected temperature values were calculated using three different equations. The troposphere temperature profile can be modeled using the equation

$$T_{Tropo} = 15.04 - .00649 \times h.$$

The lower stratosphere model is a constant

$$T_{L\_Strat} = -56.46$$

since the temperature in this range is expected to be constant. The upper stratosphere profile can be modeled using the equation

$$T_{U\_Strat} = -131.21 + .00299 \times h$$

where the temperature begins to increase. Similarly, the pressure profiles from these three atmospheric ranges can be modeled. In the troposphere, the pressure begins to decrease with altitude as shown by

$$P_{Tropo} = 101.29 \times [\frac{T + 273.1}{288.08}]^{5.256}$$

The lower stratosphere and upper stratosphere profiles show the pressure continuing to decrease as shown by

$$P_{L\_Strat} = 22.65 \times e^{1.73 - .000157 \times h}$$

and

$$P_{U\_Strat} = 2.488 \times [\frac{T + 273.1}{216.6}]^{-11.388}$$

The measured data shows the temperature decreasing as the payload rises through the troposphere, reaching a minimum temperature between -35°C and -40°C in the lower stratosphere before steadily increasing. The measured data is shifted by an average of 32°C compared to the modelled values. This is due to the expected profile being an averaged standard model of atmospheric conditions and it does not specifically represent a particular region. These models assume that the pressure and temperature values are only affected by altitude. The measured pressure profile matches the expected pressure profile during the flight through the troposphere and upper stratosphere (Figure 4b). However, the transition from the troposphere to the upper stratosphere shows a positive 2,000 Pa pressure deviation from the expected values to the measured values.

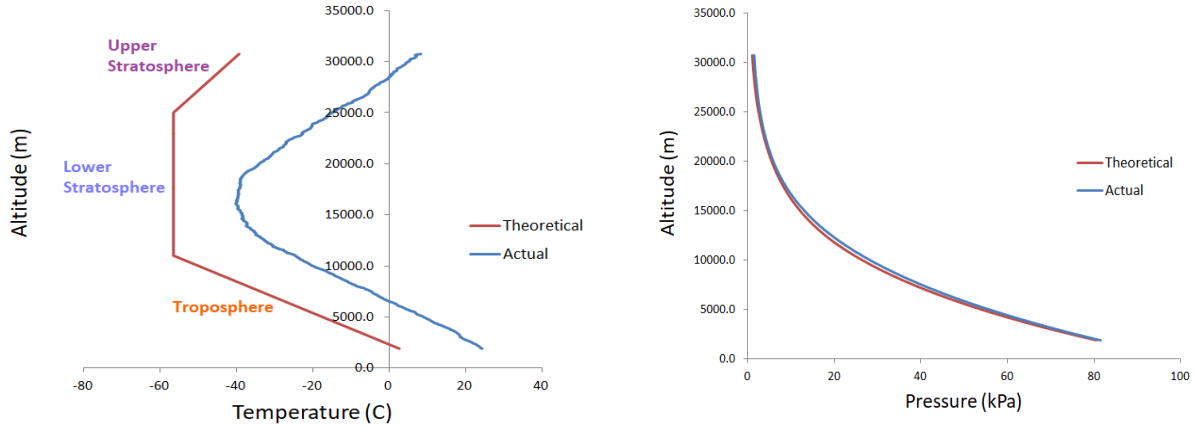

(a) **(b)**

Fig. 4 Atmospheric models compared to atmospheric data collected. (Figure 4a) graphs the temperature profiles of the troposphere, lower stratosphere and upper stratosphere. Our outside temperature data (blue) is compared to the expected values defined by current atmospheric models. (Figure 3b) Overlays the recorded absolute pressure with the calculated absolute pressure that is expected with the corresponding altitudes.

The full flight atmospheric data (Figure 5) shows a large dip in pressure associated with the balloon ascent and W shaped temperature profile with two minima that correspond to passage through the lower stratosphere on the ascent and descent. The relative humidity varies in a complex way with altitude and shows local variations in the lower troposphere.

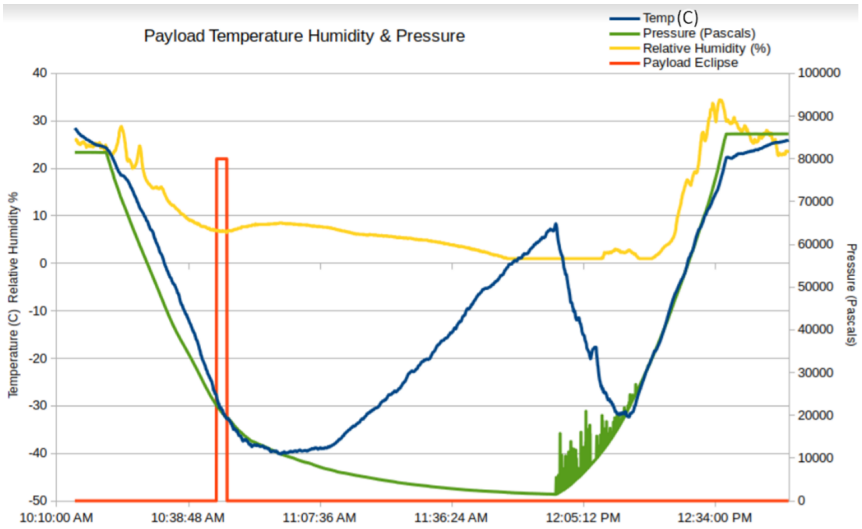

Fig. 5 Compares the temperature, relative humidity, and pressure to the eclipse event over time. Eclipse totality is represented by the spike in the red curve.

The overall pressure profile of the flight appears to fit with the expected model as shown in Figure 4b and the pressure decrease of the eclipse event is not readily apparent in the full flight data (Figure 6a) or in the *wunderground* data (Figure 7). This is a result of the eclipse–related pressure fluctuations being small compared to the overall pressure change through the flight. There is no local pressure maxima associated with totality, as seen in the ground station data (Figure 1). However, when analyzing the changes in pressure during the flight we notice an increase of pressure fluctuations after full totality (Figure 6b). It is worth noting that there are noticeable pressure fluctuations in the troposphere and in the stratosphere during the time frame of totality.

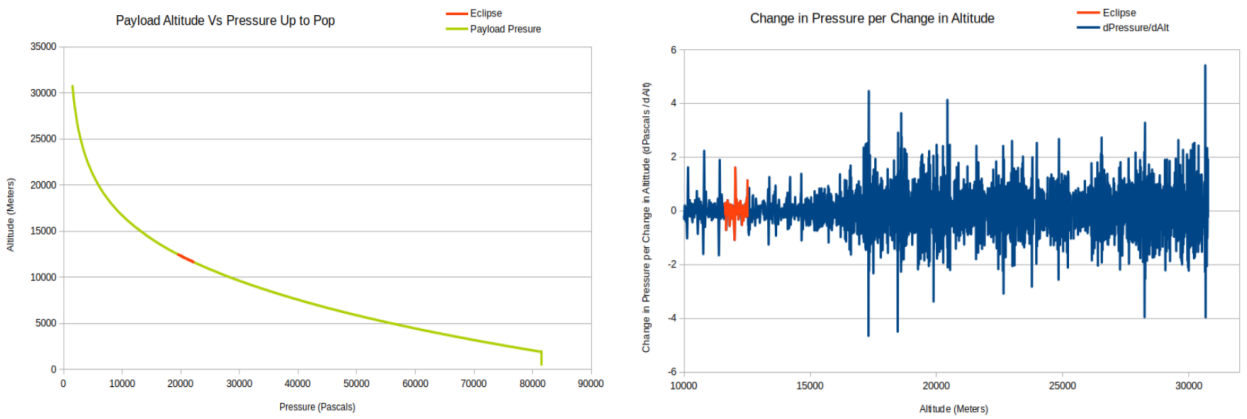

(a) **(b)**

Fig. 6 Detailed pressure measurements gathered during the eclipse. (a) plots the pressure measured during flight as a function of altitude. The red highlighted portion of the graph illustrates the eclipse event. (b) shows the change in pressure per change in altitude across the flight. The colored region representing totality shows no fluctuations.

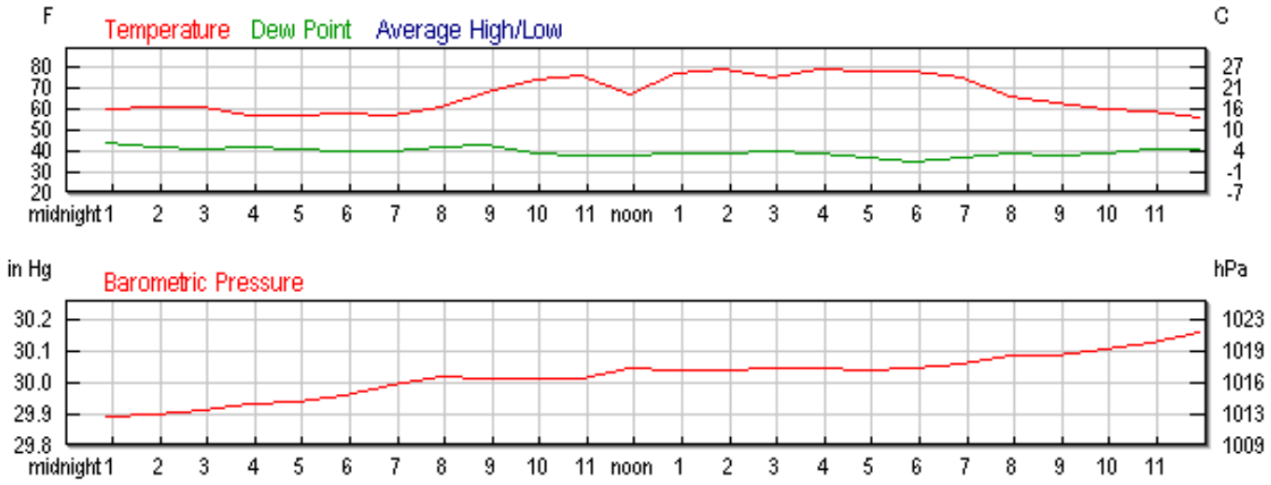

Fig. 7 Temperature, dew point and barometric pressure from *wunderground* from Douglas Wyoming on August 21, 2017.

IV. Discussion

The entire system was operating during the flight with the exception of the wind vane on the ground and the thermal imaging camera in the payload. The wind vane reported zero values during the eclipse event and the source of these errors are unknown. The thermal camera system shut down shortly after launch and did not record any images during the flight. This failure was most likely due to either a structural flaw in the power system housing or a software flaw in the app that was designed by the developer.

Overall, the weather station proved to be an essential part of our experiment since it provided context for the payload data. Since the weather station was stationary for the duration of the eclipse, we collected a well-defined light level curve indicating the behavior of the eclipse. This light curve shows that while the totality itself was 2.5 minutes, the entire event that can be seen by the human eye is 5 and a half minutes including the transition into and out of totality. We expected the transitions into and out of totality to be nearly instantaneous, but they instead occur over 1.5 minutes. Assuming a linear relation between recorded voltage and measured light, the ground station light curve implies a 95% decrease in light during the transition from the inner penumbra to the umbra. The maximum light levels measured (3.2 V) was below the maximum for the sensors (3.3 V), indicating that the sensors were not saturated at the onset of the eclipse. However, our sensors were not sensitive enough to measure light during totality. When comparing the weather station data during the Eclipse to the local weather data archived on *wunderground*[3.] we found that they had recorded similar temperature profiles during the eclipse. *Wunderground* data showed the temperature decrease from 11 A.M. to 12 P.M. even though totality and the temperature decrease occurred between 10 A.M. to 11 A.M. Glendo, WY time (as shown in our data). This 60 minute time shift is most likely due to the website's server and the time zone it is set in, however, the temperature decrease is the same for both sets of data. The lowest recorded temperature from *wunderground* right after totality at 11:53 A.M. (10:53 A.M. Glendo time) is 66.9 °F compared to our recorded temperature of 69.9 °F at the same time.

Without the weather station, the two-hour decrease in pressure during the eclipse and 20 minute pressure spike associated totality would not have been observed since the variations were small compared to pressure change over the flight. Figure 6a shows pressure as a function of altitude with the moment of totality indicated, and Figure 6b shows the change in pressure over change in altitude to magnify any fluctuations, which appears to show no visible fluctuations around totality. This suggests that the pressure spike seen on the ground did not occur in the upper troposphere between 37,000 and 40,000 ft. The barometric pressure data for Douglas (Figure 7) shows a general increase in pressure throughout the day, but without a pressure dip associated with the eclipse. The general increasing trend in pressure is consistent with our pressure measurements before and after the eclipse. Our ground-station pressure data shows an oscillation that is similar to a gravity wave, but the pattern does not appear to be a wave-like oscillation expected for a gravity wave. Our hypothesis for our totality-centered pressure spike at the ground station is that the umbra causes a localized column of sinking cold air. Although the eclipse generally caused a decrease in atmospheric pressure from

rapid cooling, our pressure data suggest that the cool dense air in and around the umbra was sinking, resulting in a highly localized and cold high-pressure feature. These effects would also be negligible at the Tropopause where the payload experienced totality. So far, we have found no reference to this effect in eclipse related literature. To further test this hypothesis, additional weather station data is needed from the path of totality.

V. Conclusion

The data collected by our payload and weather station showed the predicted temperature and pressure fluctuations as well as an unexpected pressure peak from the weather station during the eclipse. The changes in light levels measured at our ground station showed that light does not slowly diminish during the transition to full totality, but instead it decreases rapidly in the 90 seconds before full totality. The peak in air pressure associates with totality may be the result of sinking cold air, but more pressure data is needed to test this hypotheses.

VI. References

[1] C. S. Zerefos,E. Gerasopoulos, I.Tsagouri, B.E.Psiloglou, A.Belehaki, T. Herekakis, A. Bais, S. Kazadzis, C. Eleftheratos, N. Kalivitis, and N. Mihalopoulos. (2007). Evidence of gravity waves into the atmosphere during the March 2006 total solar eclipse. Atmos. Chem. Phys. Discuss. vol. 7, May. 2007, pp. 4943-4951

[2] Hall, N., ed., "Earth Atmosphere Model," NASA Glenn Research Center
Available: https://www.grc.nasa.gov/www/k-12/airplane/atmosmet.html

[3] Marty, J., Dalaudier, F., Ponceau, D., Blanc, E., and Munkhuu, U., "Surface Pressure Fluctuations Produced by the Total Solar Eclipse of 1 August 2008," American Meteorological Society, vol. 70, Mar. 2013, pp. 809–823.

[4] Maturilli, Marion & Ritter, Christoph. (2016). Surface radiation during the total solar eclipse over Ny-Alesund, Svalbard, on 20 March 2015. Earth System Science Data. 8. 159-164. 10.5194/essd-8-159-2016.

[5] wunderground, "Weather History for KDGW," wunderground.
Available:https://www.wunderground.com/history/airport/KDGW/2017/8/21/DailyHistory.html?req_city=&req_state=&req_statename=&reqdb.zip=&reqdb.magic=&reqdb.wmo=